# Proton Directed Flow in Beam Energy Scan II

Emmy Duckworth for the STAR Collaboration (educkwor@kent.edu), Kent State University

Supported in part by:
U.S. DEPARTMENT OF ENERGY Office of Science

The STAR Collaboration
https://drupal.star.bnl.gov/STAR/presentations

# Beam Energy Scan

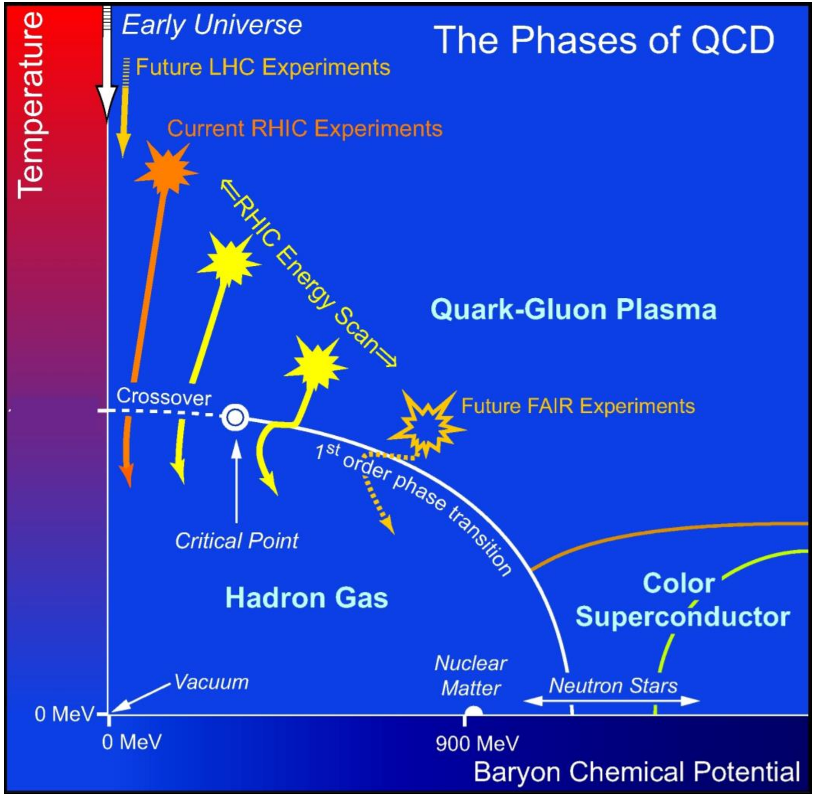


- STAR Beam Energy Scan gives us access to a wide sweep of phase space to search for critical point and to understand the QCD phase structure
- Hydro and nuclear transport models suggest that $v_1$ offers sensitivity to the dynamics of the expanding medium
- Proton flow is predicted to be sensitive to the softening of the equation of state near a first order phase transition

# Motivation

- In BES-I we saw a nonmonotonic trend in the proton $v_1$ slope vs collision energy
  - Occurring much higher than expected

- Proton $v_1$ is driven by 2 different sources:
  - The initial protons that are baryon sources
  - The protons generated during the collision

$$v_1 = \langle \cos(\phi - \Psi_{ep}) \rangle$$

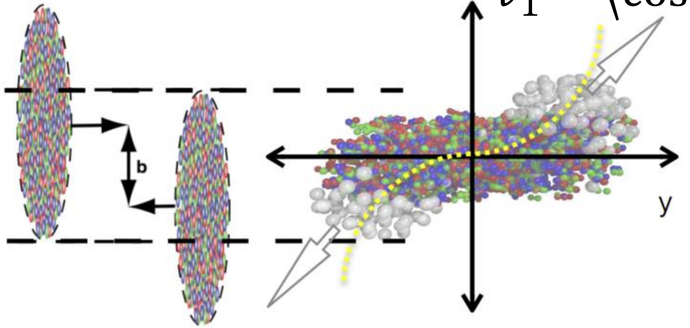


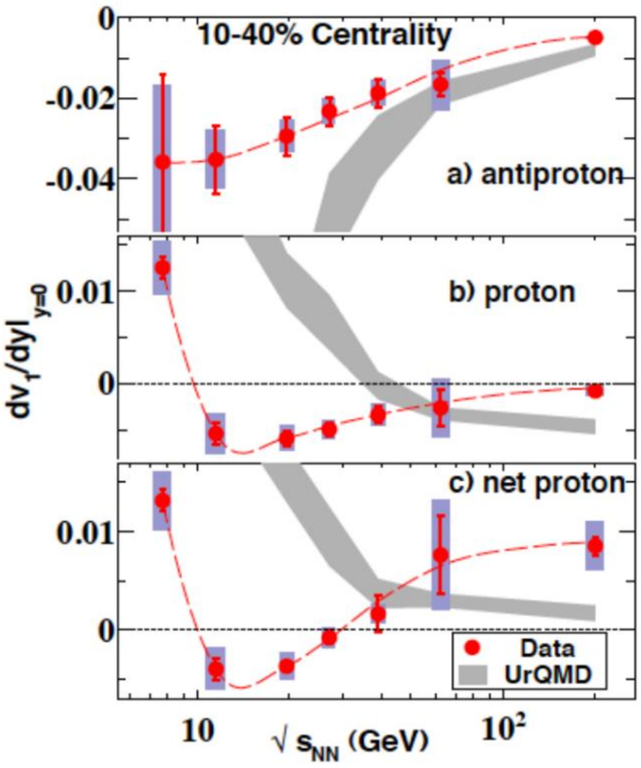


(PRL 112, 162301 (2014))

# Motivation

- To capture this behavior, net proton $v_1$ was defined as:

$$N_p v_{1,p} = N_{p,produced} v_{1,produced} + (N_p - N_{\bar{p}}) v_{1,net}$$

- We assume $N_{p,produced} v_{1,produced} = N_{\bar{p}} v_{1,\bar{p}}$ and solve:

$$v_{1,net} = \frac{(v_{1,p} - r v_{1,\bar{p}})}{1 - r}$$

(r is the yield ratio of anti-protons to protons)

- Net proton $v_1$ slope at mid-rapidity also exhibits non-monotonic behavior in the same region

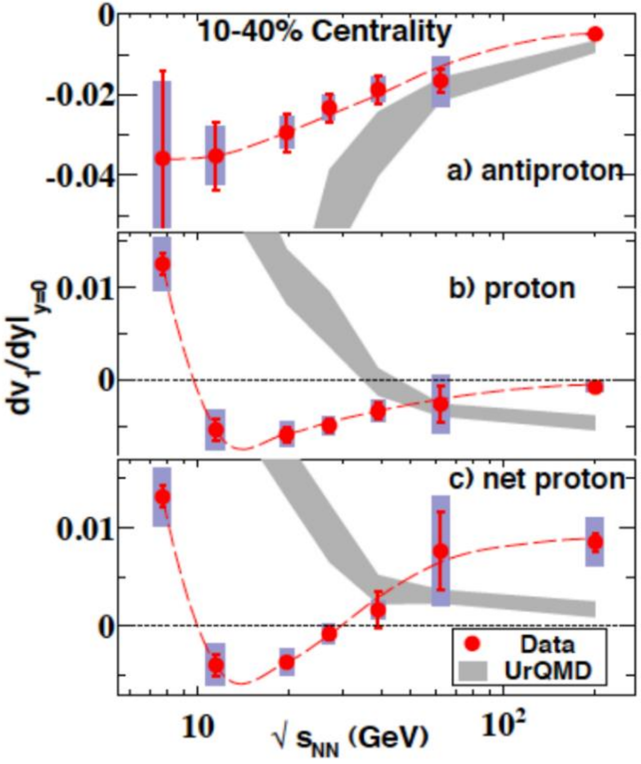


(PRL 112, 162301 (2014))

# Motivation

- Driving phenomena behind Proton $v_1$:
  - Interaction between hadrons in the initial compression stages contributes to positive flow
  - Tilted matter produces negative flow in expansion stage

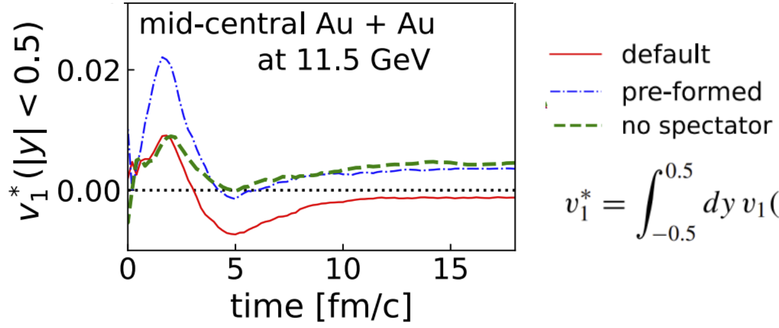


$$v_1^* = \int_{-0.5}^{0.5} dy\, v_1(y)\,\mathrm{sgn}(y).$$

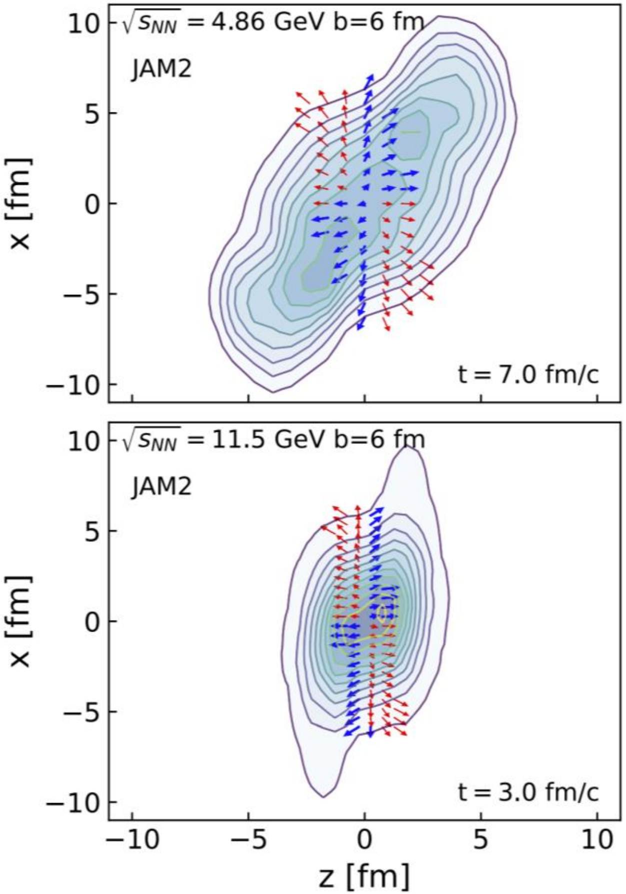


Baryon density distribution for Au+Au collisions, blue arrows indicate flow, red arrows antiflow.
Phys. Rev. C 105, 014911 (2022)

# Anti Proton $v_1$ as a Proxy for Medium Flow

- Initial geometry values scaled to match the $v_1$ in 10-20% centrality

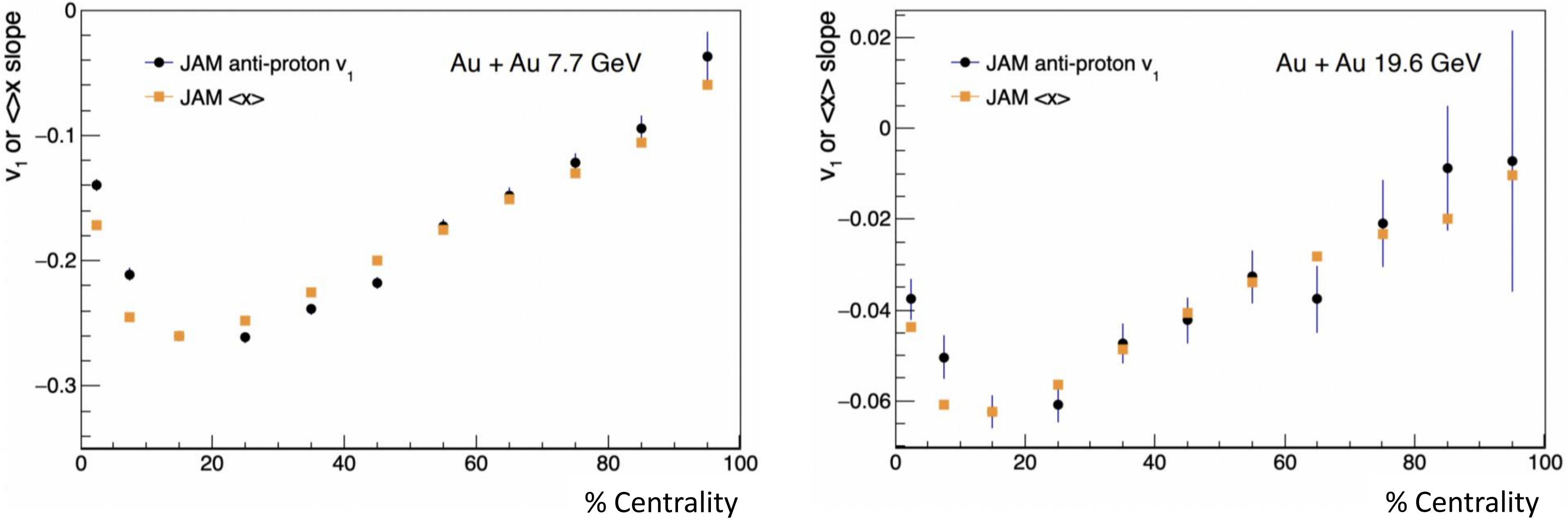


- Initial geometry largely captures the centrality dependence of anti-proton $v_1$
- Agrees very well in JAM
- Reflects origin from medium response to initial geometry

# Motivation

- Thus, we can instead break it down to the initial interactions and the medium expansion:

$$N_p v_{1,p} = N_p v_{1,medium} + (N_p - N_{\bar{p}}) v_{1,excess}$$

- Assuming $v_{1,medium} = v_{1,\bar{p}}$ gives:

$$v_{1,excess} = \frac{(v_{1,p} - v_{1,\bar{p}})}{1-r} \quad \left(\text{vs. } v_{1,net} = \frac{(v_{1,p} - r v_{1,\bar{p}})}{1-r}\right)$$

- Let us see how this new observable behaves

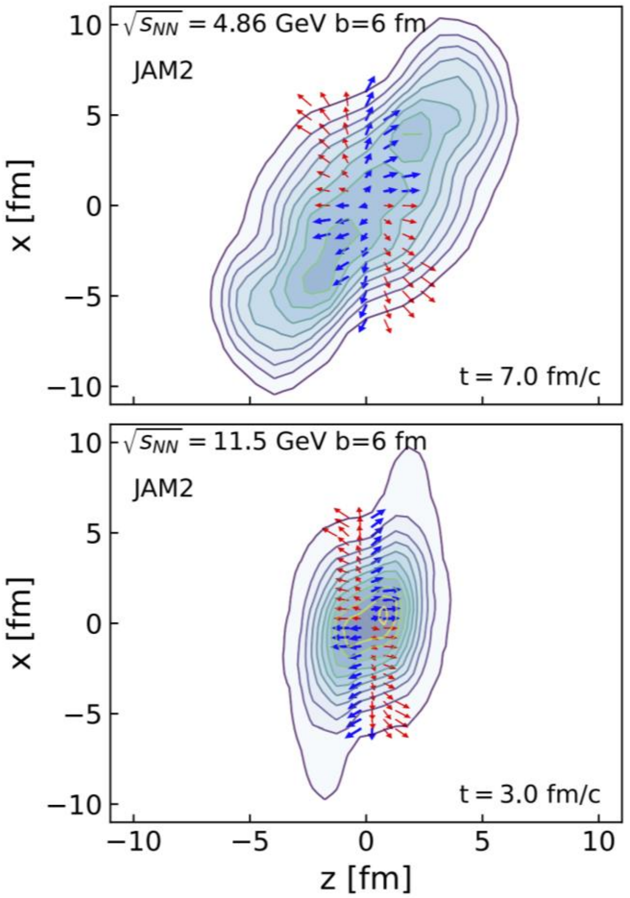


Baryon density distribution for Au+Au collisions, blue arrows indicate flow, red arrows antiflow.
Phys. Rev. C 105, 014911 (2022)

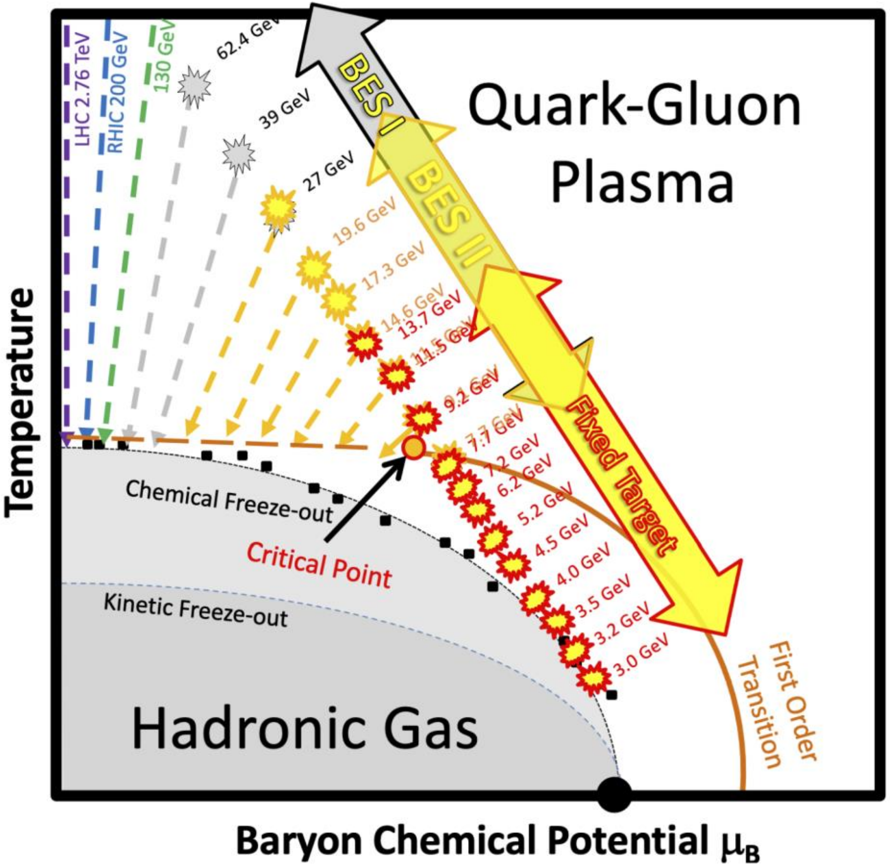


https://doi.org/10.1016/j.nuclphysa.2017.05.042

# BES-II Dataset

- We are using the BES-II dataset:
  - 10x the statistics of BES-I
  - Upgraded detector to include the EPD, iTPC, and eTOF
- Ranges from $\sqrt{s_{NN}}$ =3.0 GeV (Fixed target) up to 27 GeV (collider mode)
- Extends the $\mu_B$ range to 200 – 420 MeV
  - Up to 720 MeV with FXT

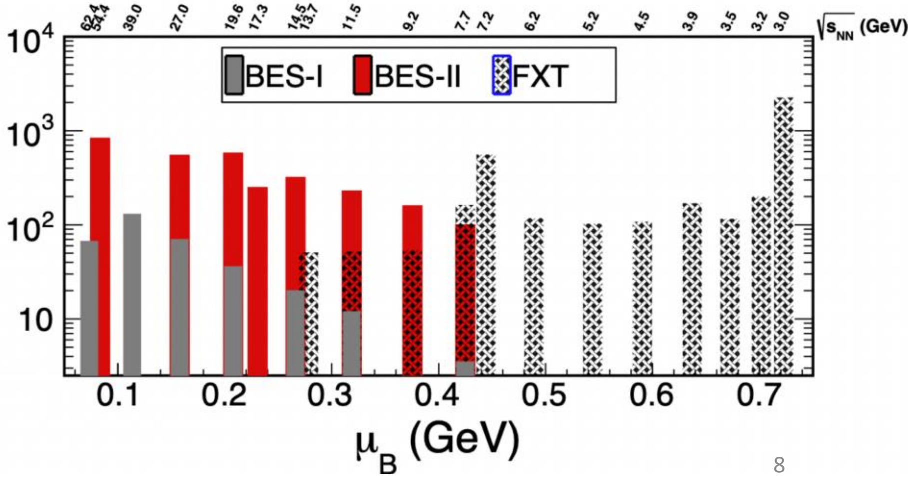

# STAR Detector Upgrades

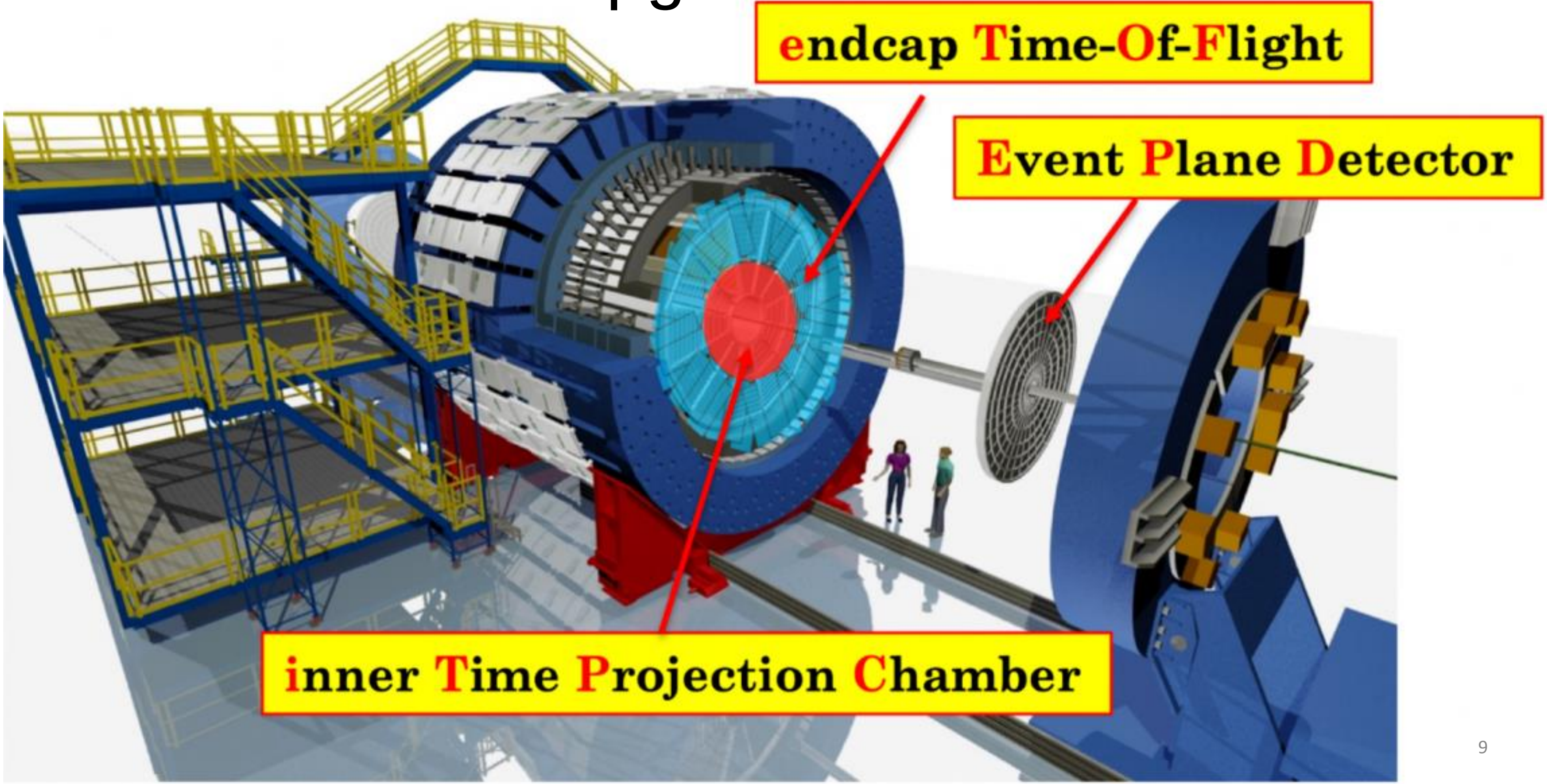

# Event Plane Detector

- Pseudorapidity range: 2.1 to 5.1
- 372 tiles are Eljen scintillators
- Significantly increased Event plane accuracy as compared to Beam-Beam Counters (BBC)

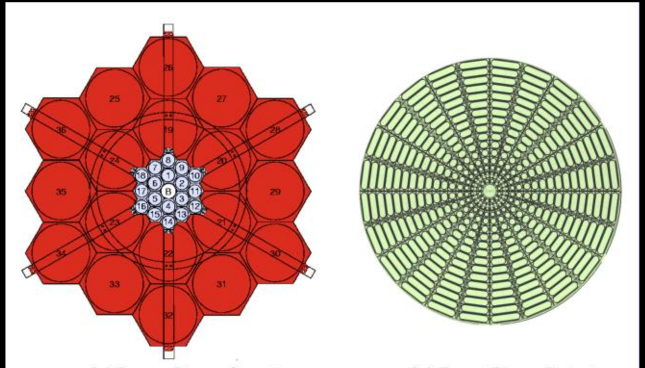
(a) Beam-Beam Counters (b) Event Plane Detector

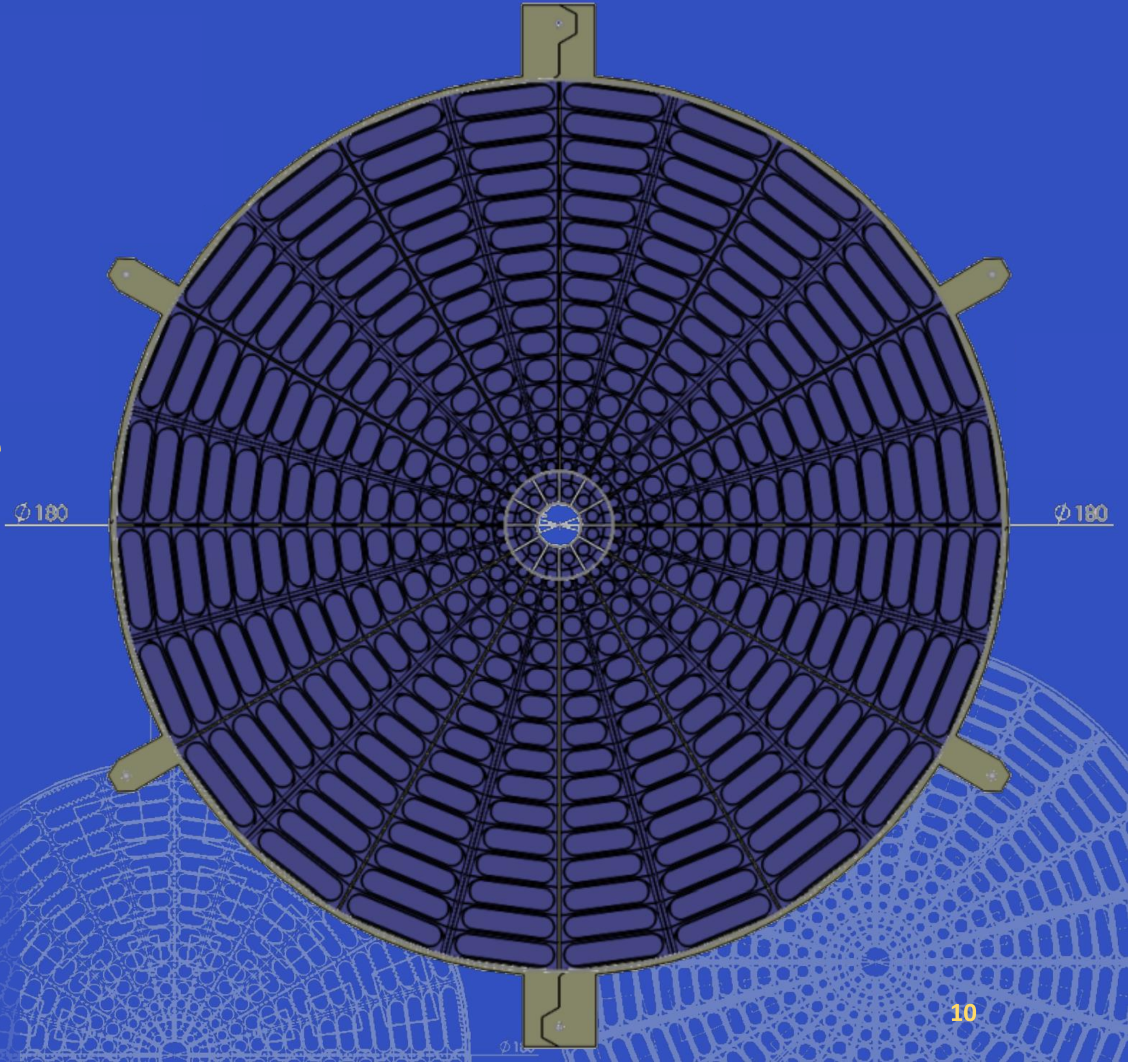

# Procedure

- Measure the event plane angle for each event

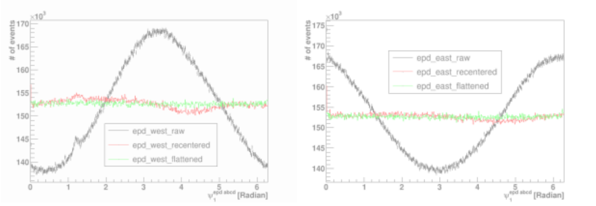


- Identify the (anti)protons from the collision

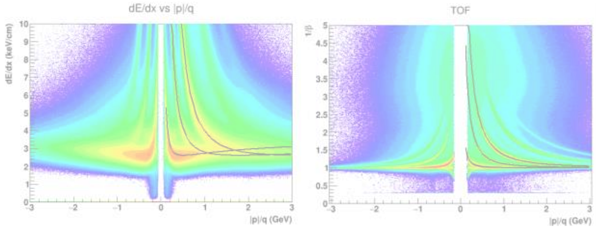


- Measure the $v_1$ of (anti)protons and calculate excess $v_1$

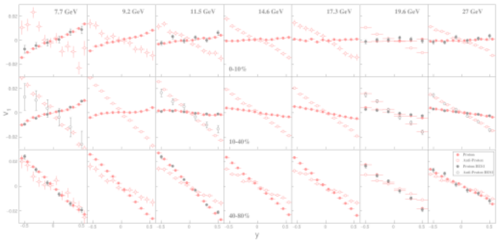

# Event Plane Determination

- The event plane is measured by the EPD based on number of Minimally Ionizing Particles (nMIP)

$$\vec{Q} = \sum_{i \in tile} w_{x,i} \cos\phi_i \,\hat{x} + w_{y,i} \sin\phi_i \,\hat{y}$$

- We then recenter the event plane

$$\vec{Q}_{recentered} = -\left\langle \vec{Q} \right\rangle_{run} + \sum_{i \in tile} w_{x,i} \cos\phi_i \,\hat{x} + w_{y,i} \sin\phi_i \,\hat{y}$$

- Then flatten the event plane distribution

$$\phi_{EP} = \sum_{n=1}^{20} \frac{-2}{n} \langle \sin n\phi_Q \rangle_{run} \cos n\phi_Q + \frac{2}{n} \langle \cos n\phi_Q \rangle_{run} \sin n\phi_Q$$

Ref: Phys.Rev.C 58 (1998) 1671-1678

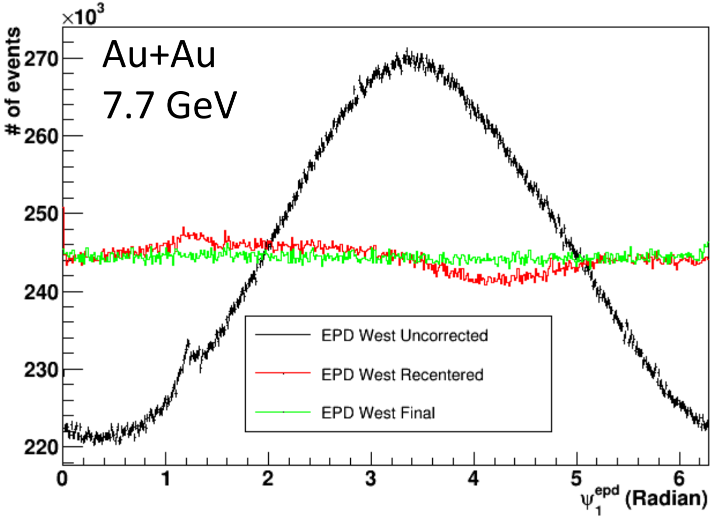


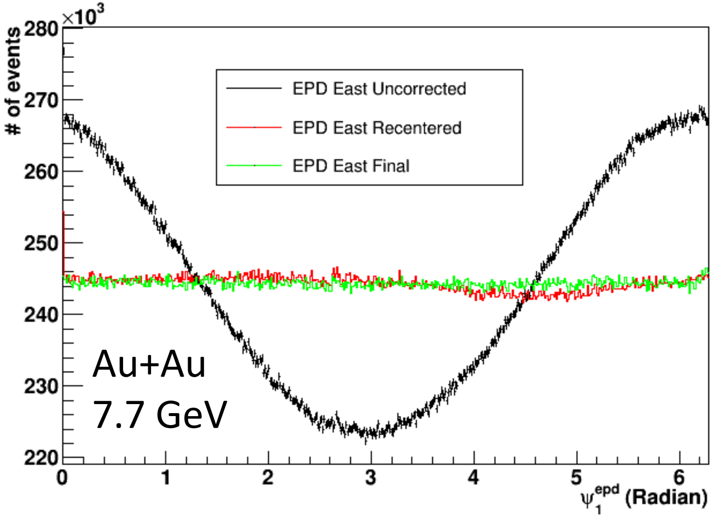

# Resolution

$$\vec{Q} = \hat{x} \sum_{i \in tile} w_i \cos \phi_i + \hat{y} \sum_{i \in tile} w_i \sin \phi_i$$

$$w_i = w(nMIP) * v_{1,raw}(\eta)$$

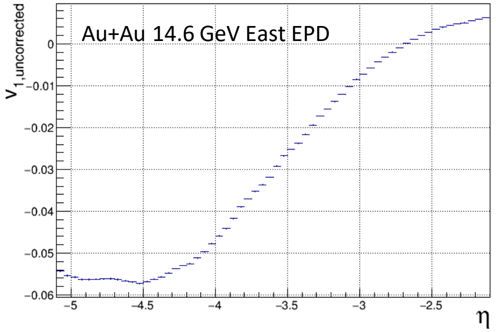


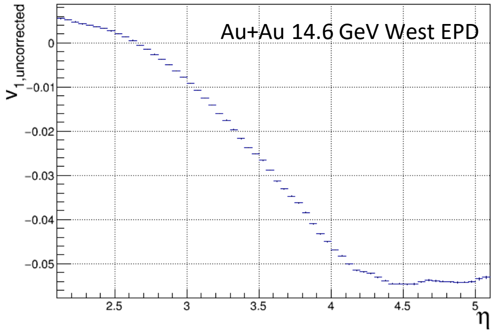


- For 9.2 to 27 GeV, there is a sign change of $v_1$ in the region of the EPD, lowering resolution
- To Correct for this, we can add an additional weighting factor based on the raw $v_1$ vs. η
- This η weighting is highly effective at increasing event plane resolution
- Gives significantly higher resolution than BES-I

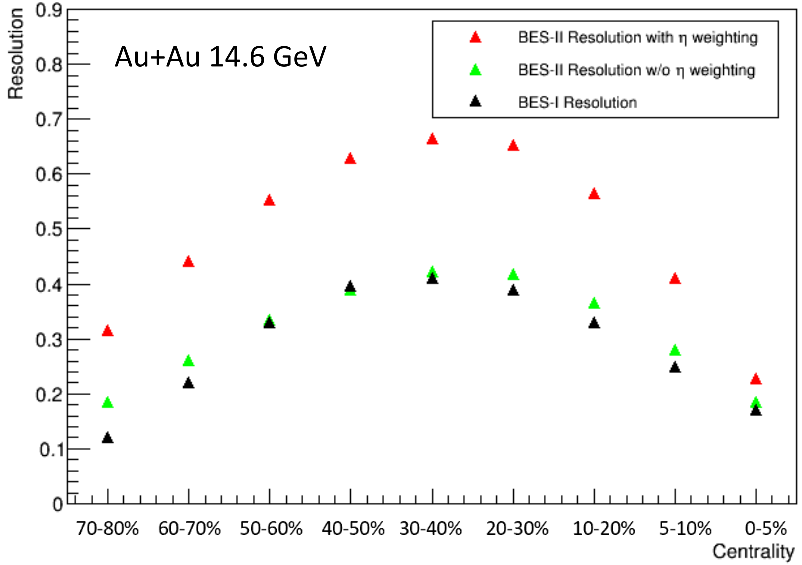

# Particle Identification

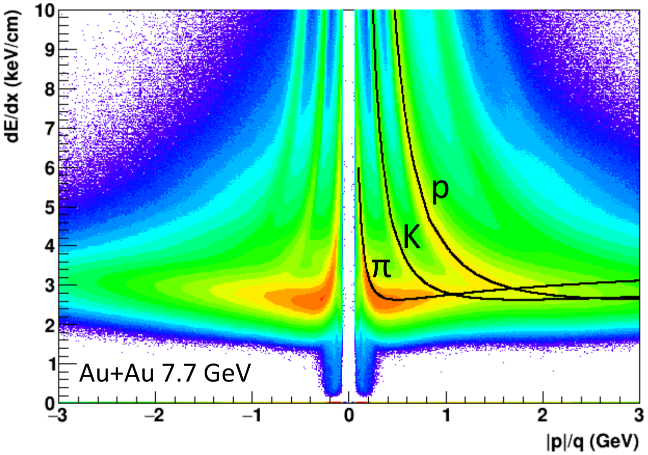


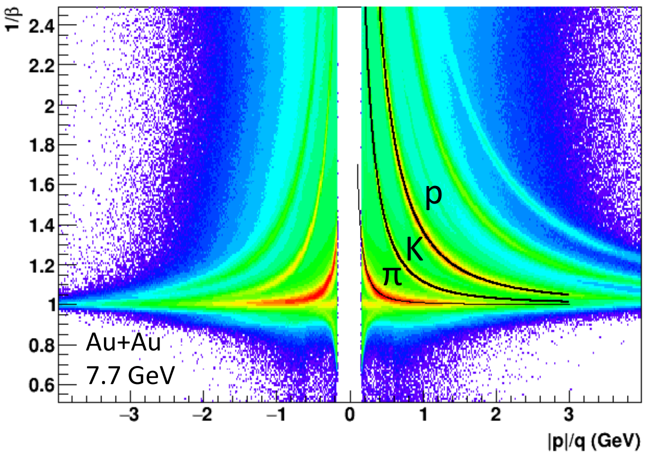


PID is:

- Require TOF: $0.8 < \text{mass}^2 < 1.0$ GeV$^2$
- $|N\sigma_{dE/dx}| < 3.0$ Relative to expected dE/dx value

- Both Proton and antiproton have high purity signals

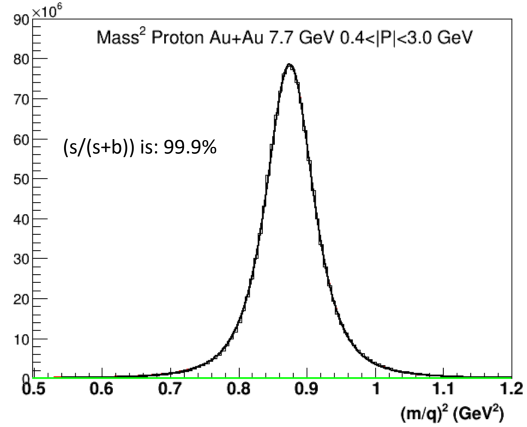


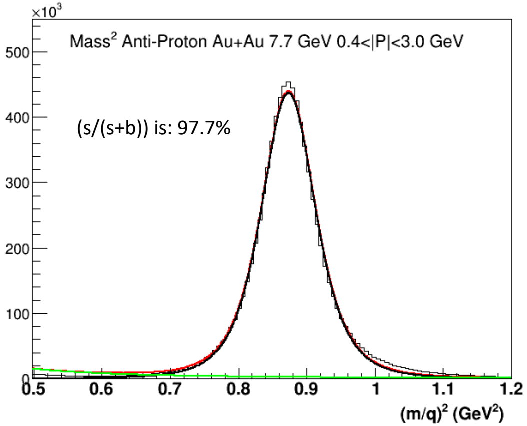

# Acceptance

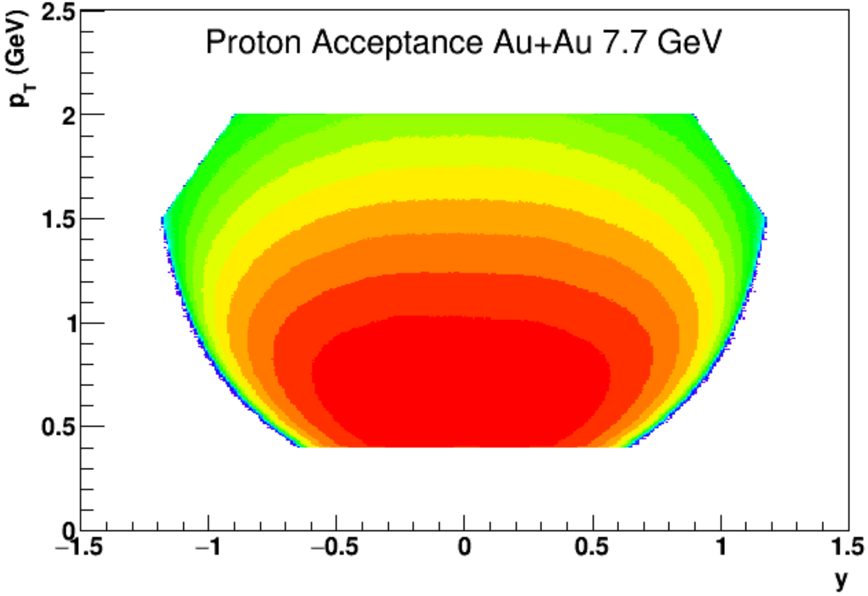


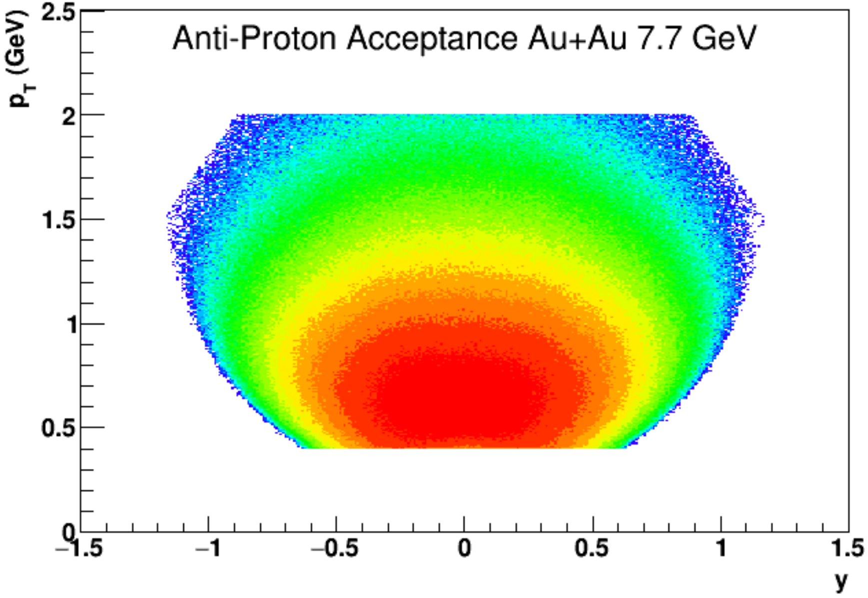


We see that we have good acceptance in the mid rapidity window (-0.5<y<0.5)

# BES II Proton and Anti-Proton Directed Flow

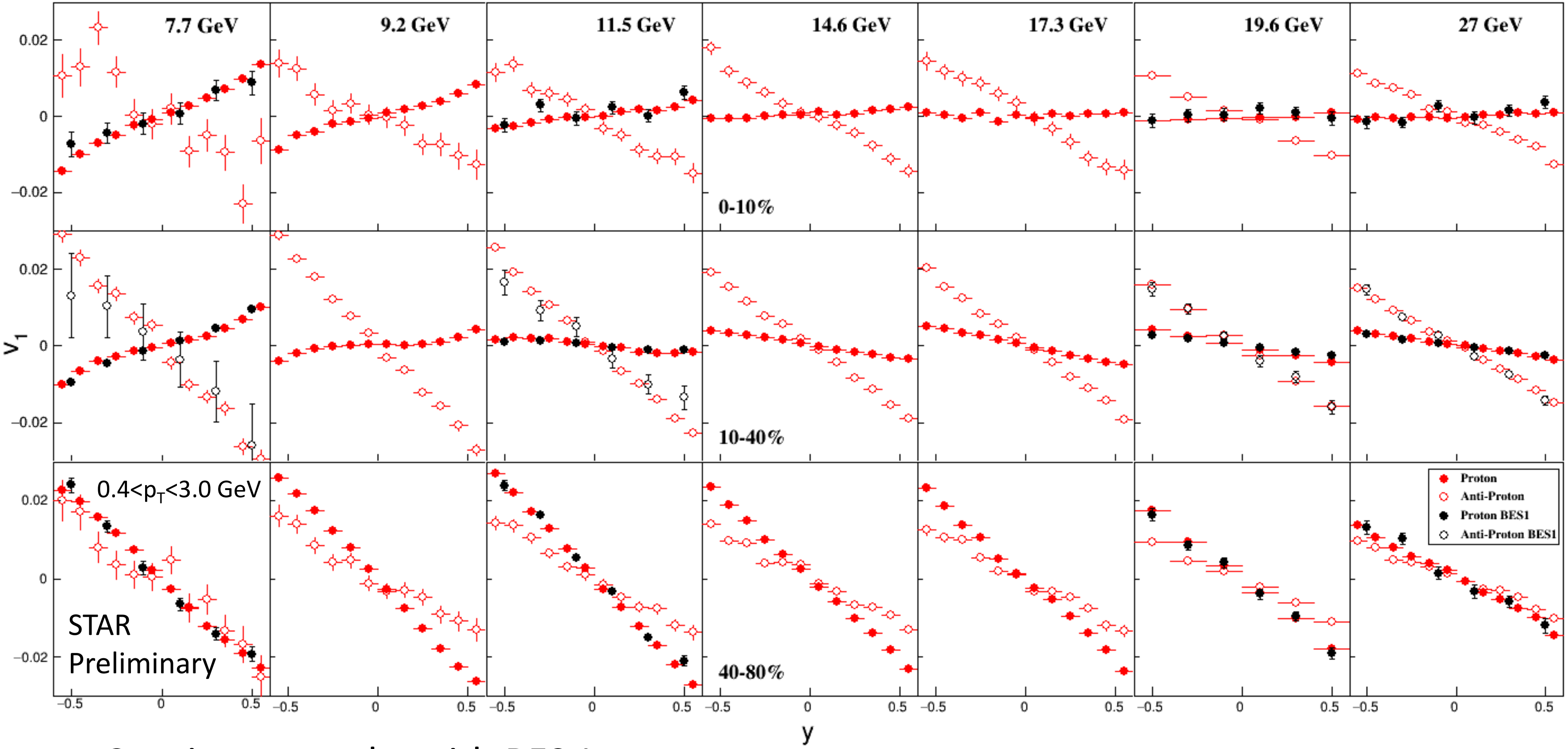


- Consistent results with BES-I
- Slope is extracted by using a linear fit over -0.5<y<0.5

# BES-I to BES-II Comparison

- BES-II Fit is linear over range -0.5<y<0.5
  - -0.8<y<0.8 for BES-I
- Significantly more accurate anti-proton results with the BES-II data
- Proton systematic error for BES-II dominated by cubic fit at low energies
- Proton statistical Error reduced by factor of 7

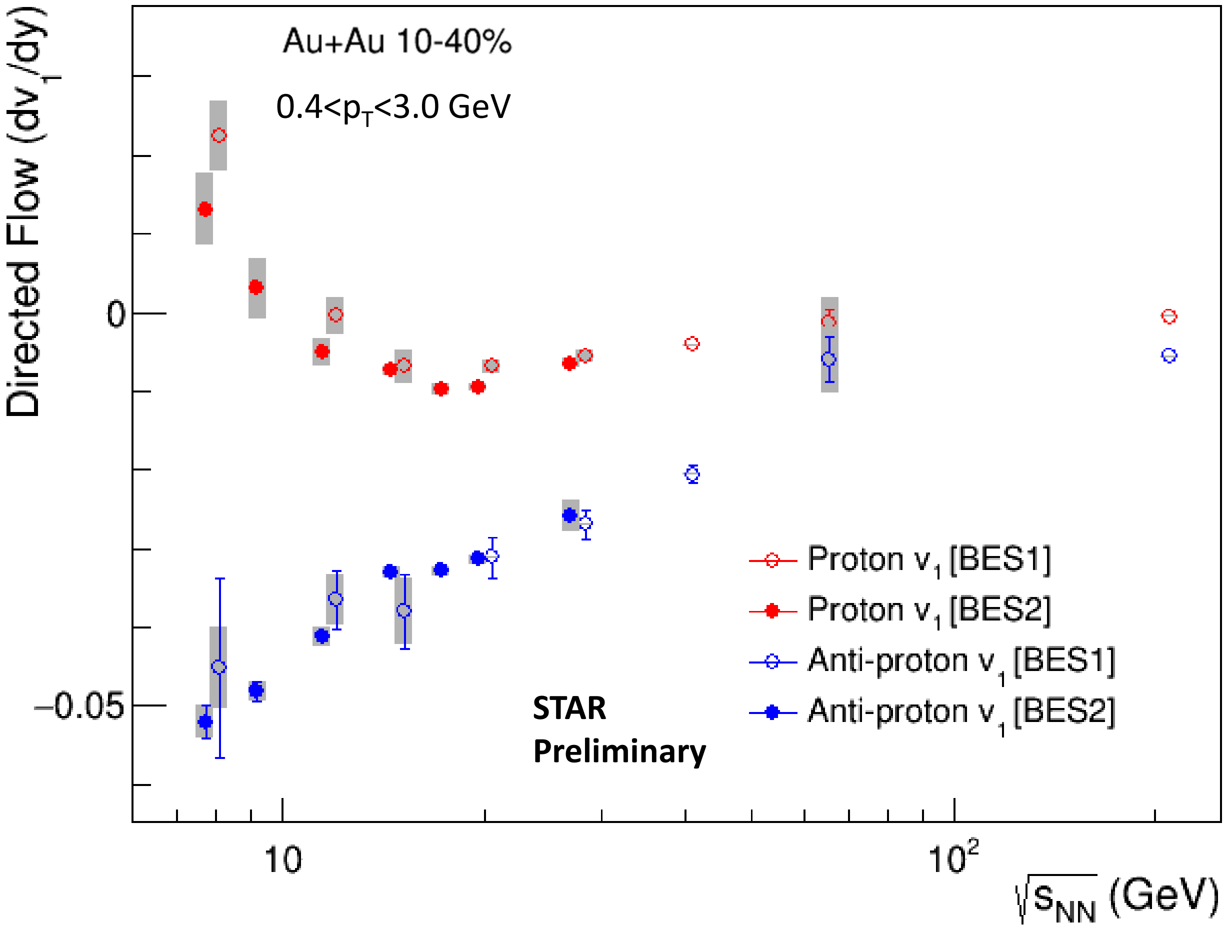

# Collision Energy Dependence

$$N_p v_{1,p} = N_p v_{1,medium} + (N_p - N_{\bar{p}}) v_{1,excess}$$

$$y_{beam}(\sqrt{s_{NN}}) = \cosh^{-1}(\sqrt{s_{NN}}/m_p)$$

- Clear scaling of excess Proton flow with collision energy

- Scaling starts to break at 11.5 GeV

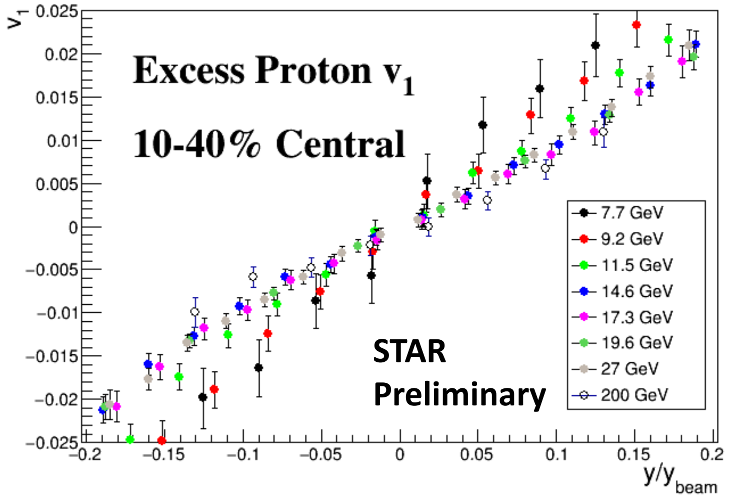


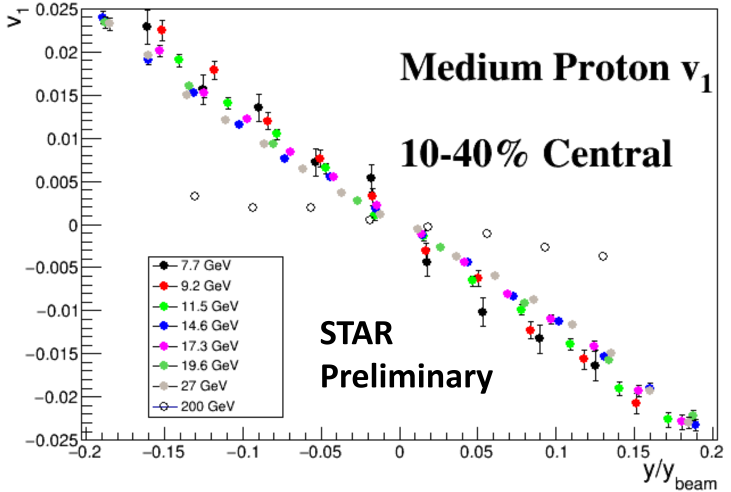

# Comparisons with JAM model: Cascade and Meanfield

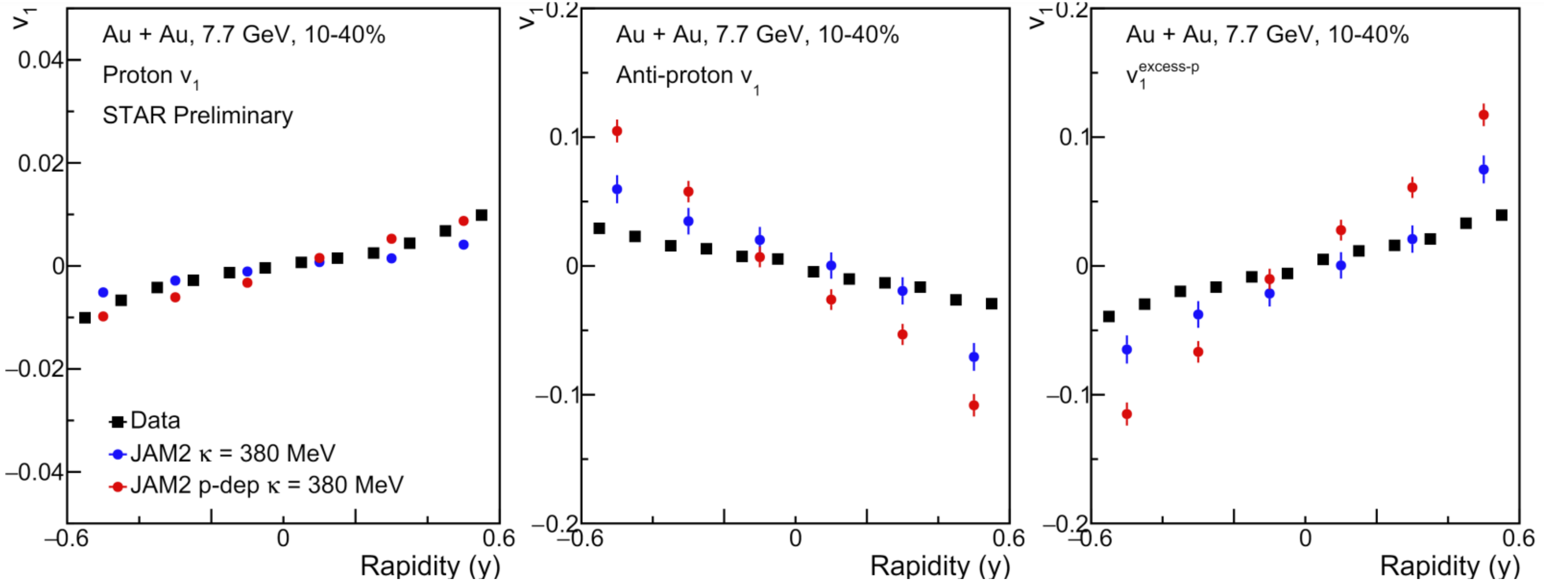


- Vastly different values for the two components between different modes, but proton $v_1$ similar
- More sensitivity to change in medium dynamics/EoS than just looking at proton $v_1$

# Model Comparison

- Models fail to show the scaling behavior above 14.6 GeV
- Below 14.6 GeV models overpredict the magnitude of the data
- Adding momentum dependence to the potential increases this overprediction

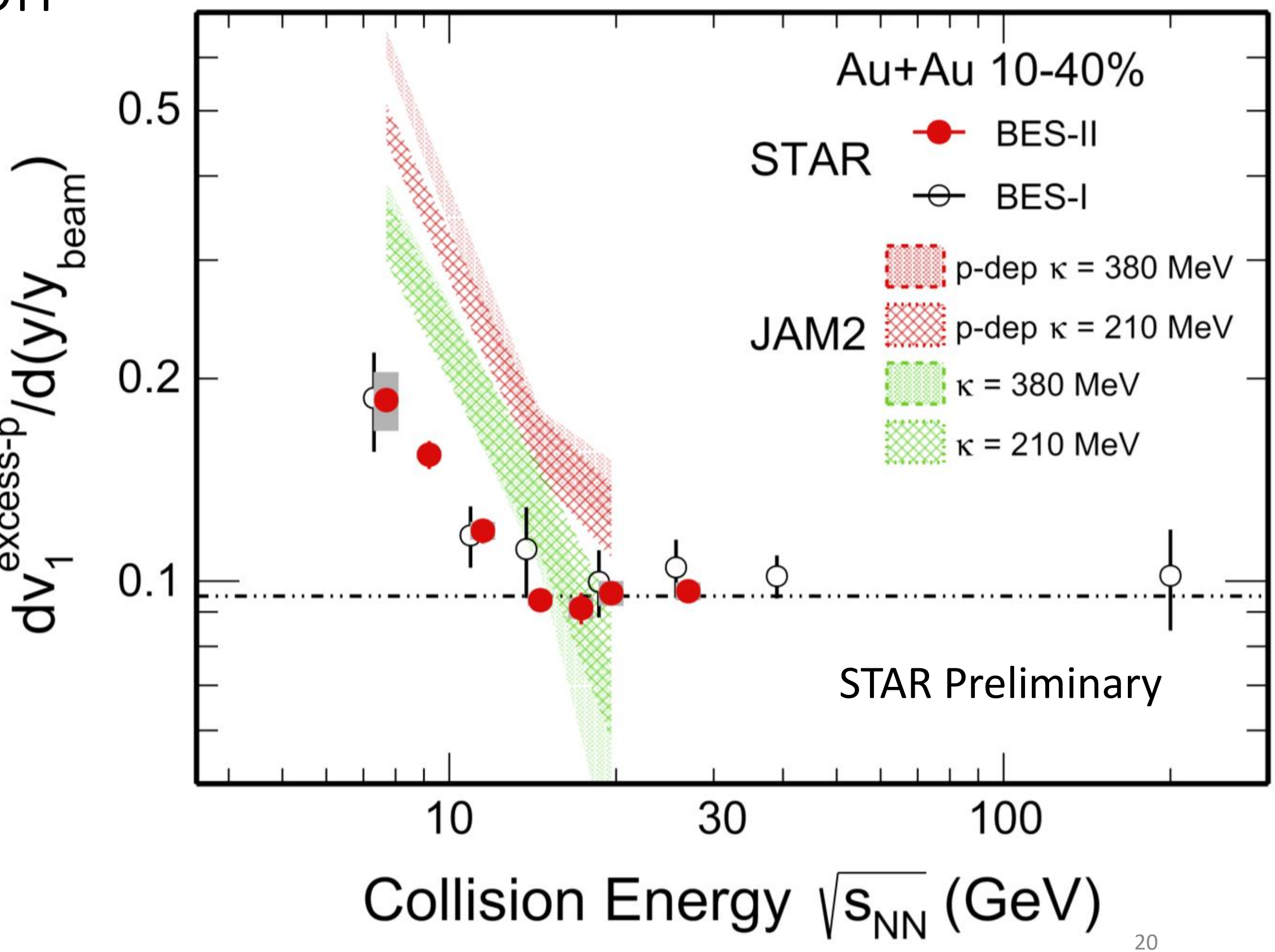

# Summary

- Precision measurement of proton and antiproton $v_1$ from 7.7 to 27 GeV
- Excess $v_1$ of transported protons vs $y/y_{beam}$ is constant from 200 — 14.6 GeV
- Deviates from scaling at 11.5 GeV and below — change in medium/collision dynamics
- Mean field calculations overpredict the data, even for the softest EoS
  - New data expected to offer better constraints on EOS parameters

# Thank you!

# Backup

# Excess Proton Flow and Net Proton Flow

- BES-II Fit is linear over range -0.5<y<0.5
  - -0.8<y<0.8 for BES-I
- We see monotonic behavior in excess proton flow
- This behavior scales with beam rapidity from 14.6 GeV to 200 GeV
- Net-Proton systematic error for BES-II dominated by cubic fit at low energies
  - This check was not included for BES-I

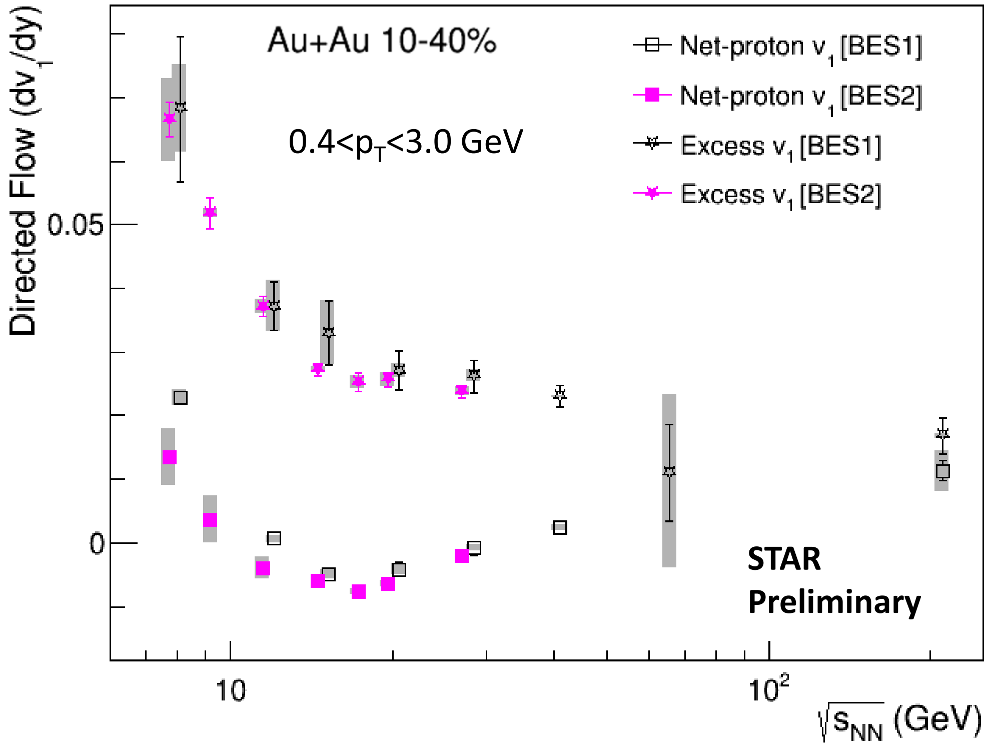

# Energy dependence of $v_1$ slope

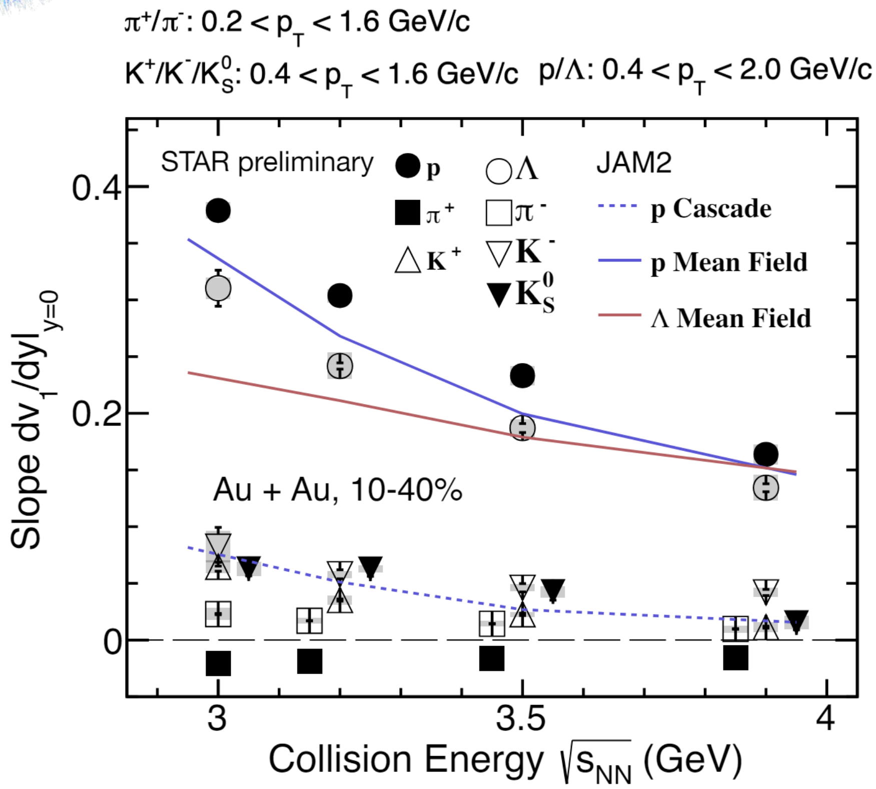


1) $v_1$ slope of baryons drops as collision energy increases
2) JAM with baryonic Mean Field better describe data
   - Mean field potential play important role

# PID Purity

- Signal purity decreases at higher momentum so its important to check
- At 7.7 GeV up to 11.5 GeV the anti-proton signal is not pure enough to just to sum up identified tracks.

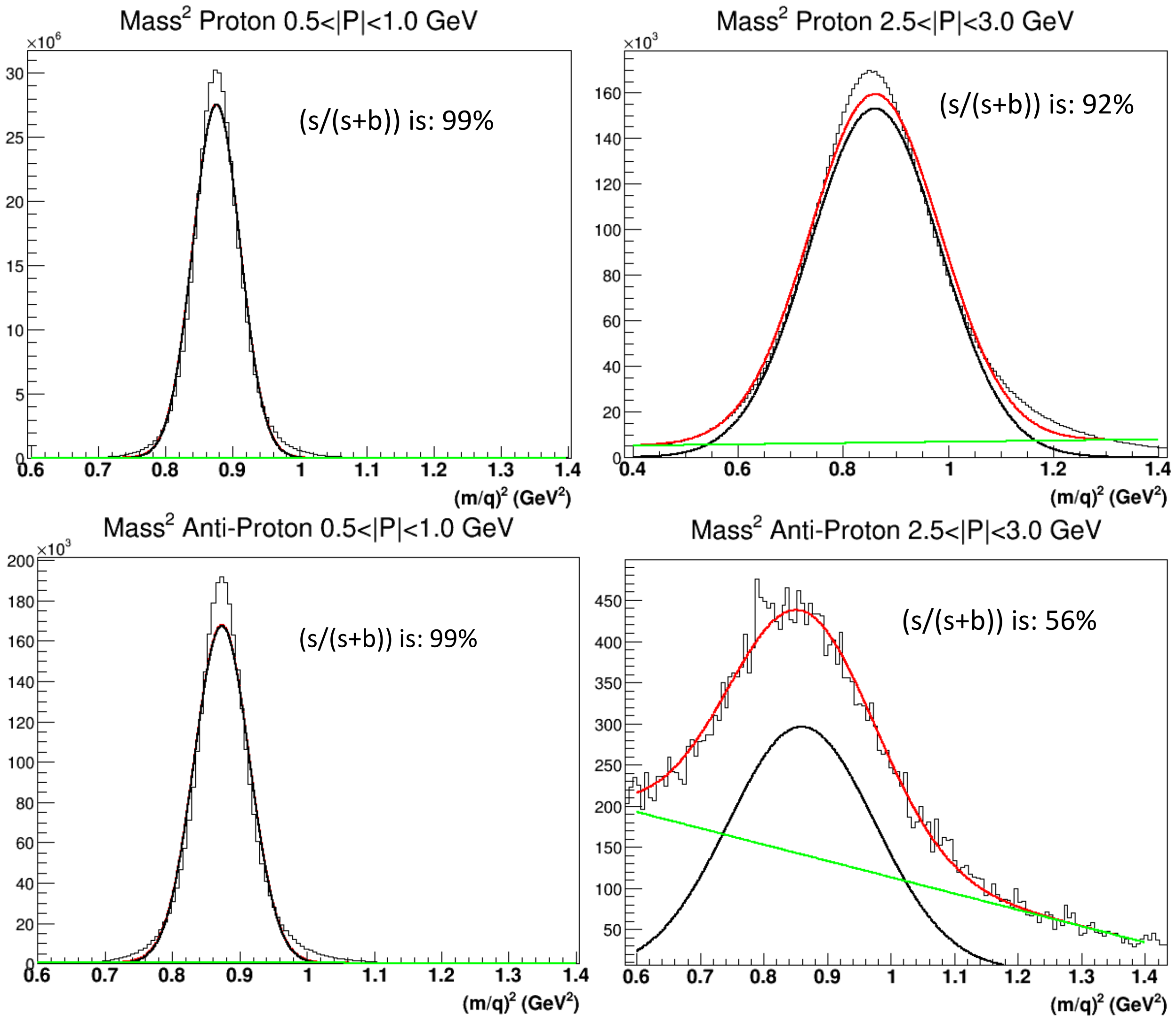

# Background subtraction of Anti-Proton signal

- The $mass^2$ of tracks satisfying the <dE/dx> PID were divided into bins based on centrality, y, $\phi$-$\psi_r$, and |P|.
- The signal and background of $mass^2$ was then measured for each.
- Then the signals were combined over |P| to get the signal vs $\phi$-$\psi_r$ in 10 different rapidity windows.

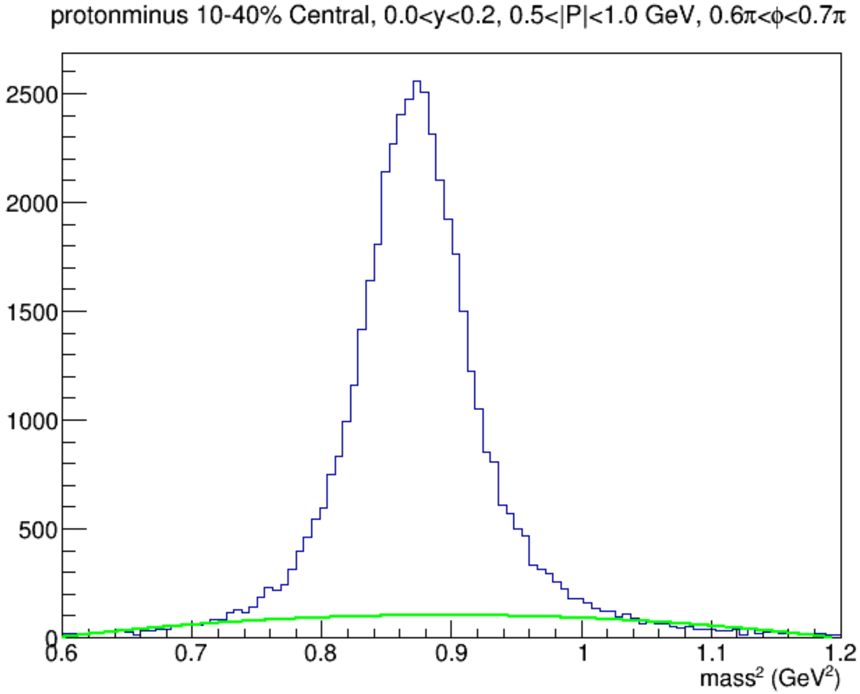

# RQMD Modeling

- Idea is to use classical Hamiltonian formalism
- We start with 8N phase space variables and reduce them with 2N constraints:
  - On-mass-shell constraint (gives N constraints)
  - Time fixation (gives N-1 constraints)
  - Define evolution temporal parameter t (gives 1 constraint)
- Each one of these constraints can be written as an equation $\phi_i = 0$, and so the Hamiltonian consists of the constraint conditions with their lagrange multipliers.

$$H = \sum_{i=1}^{2N-1} u_i \phi_i$$

For RQMD/S the on-mass-shell constraint is: $\phi_i = p_i^2 - m_i^2 - 2m_i V_i$

For RQMDs and RQMDv: $\phi_i = (p_i - V_i)^2 - (m_i - S_i)^2$

# 200 GeV

- Model prediction of flow at 200 GeV turns negative
- This further suggests a change in the equation of state

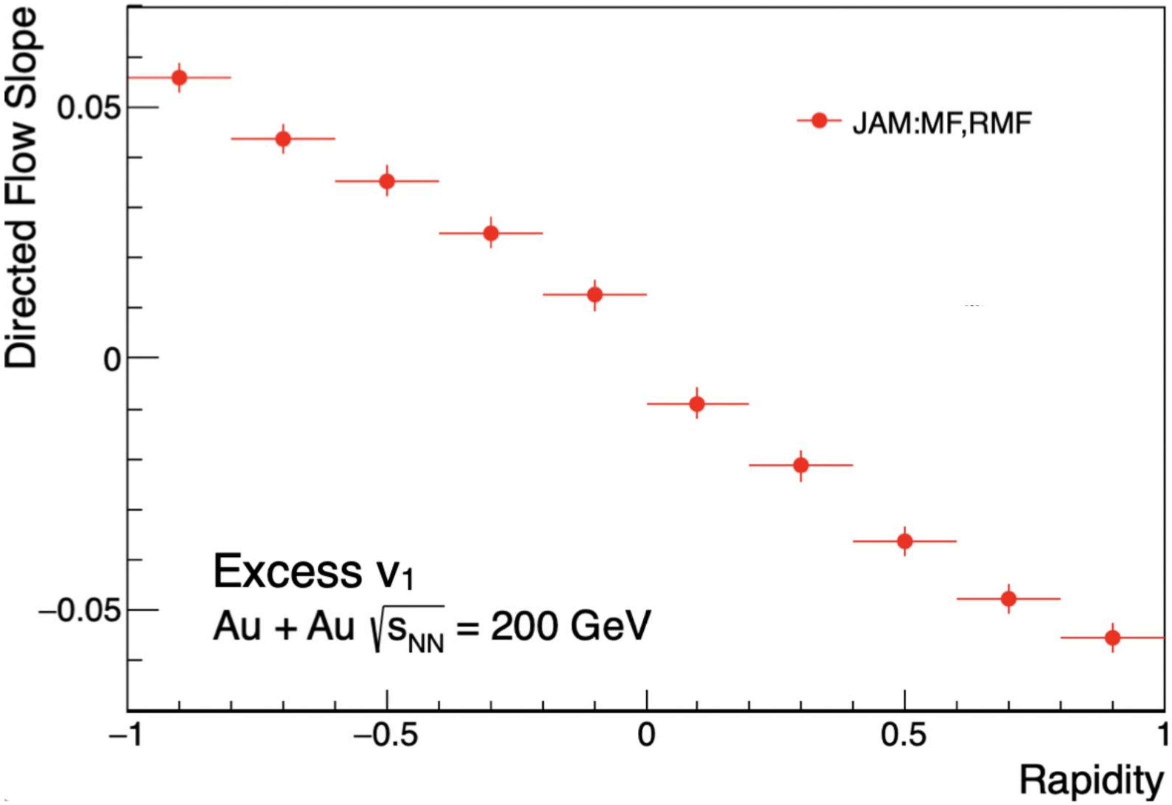

# Time Dependent Flow



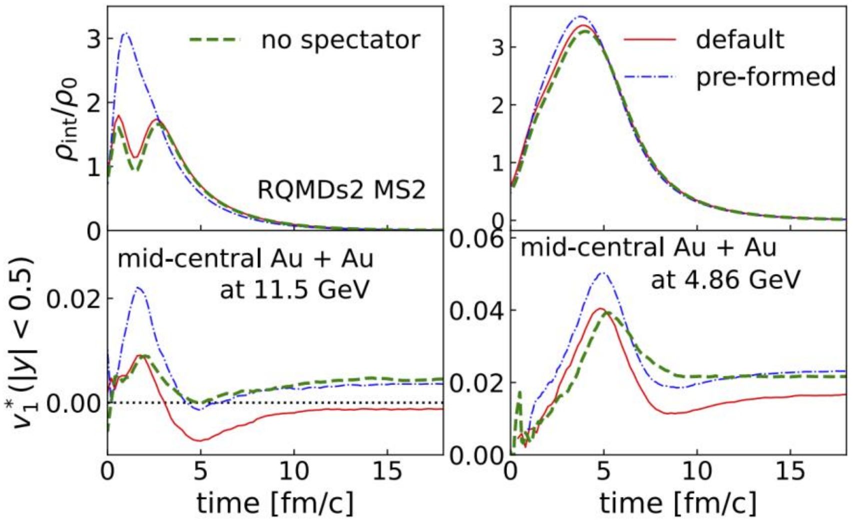


FIG. 6. Time evolution of the invariant interaction density (upper panel) averaged over the central cell of $|x| \leqslant 3$ fm, $|y| \leqslant 3$ fm, and $|z| \leqslant 1$ fm, and sign weighted directed flow $v_1^*$ of baryons at mid-rapidity $|y| < 0.5$ (lower panel) for mid-central Au + Au collisions at $\sqrt{s_{NN}} = 11.5$ GeV from the RQMDv2 calculation are shown in the left panels. Right panels show the same but for the beam energy of 4.86 GeV. The solid lines show the results from default calculations. The dotted-dashed lines show the results of the calculations that include the potential interaction for pre-formed baryons. The dashed lines represent the results of the calculation without interactions of spectator matter.

# Directed Flow ($v_1$)

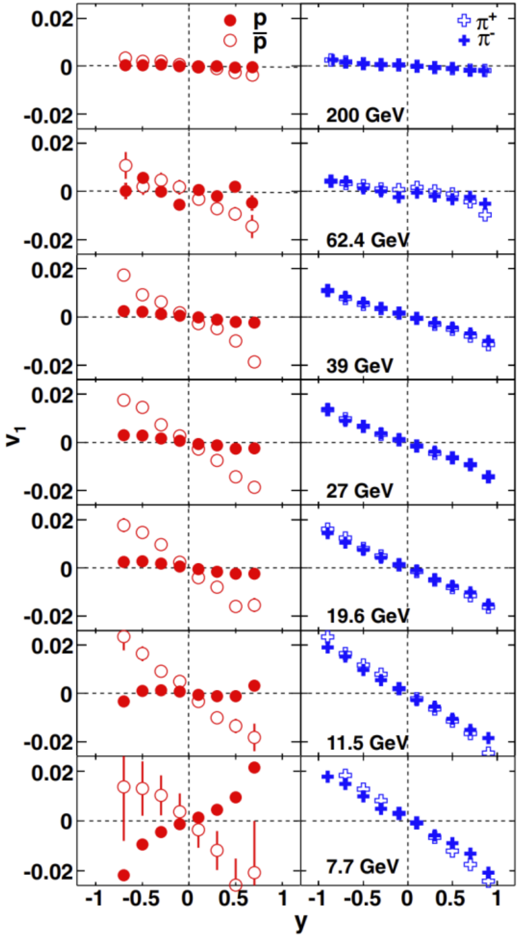


Directed flow of protons and pions from BES-I (PRL 112, 162301 (2014))

- Hydro and nuclear transport models suggest that $v_1$ offers sensitivity to the dynamics of the expanding medium
- Proton flow is believed to be sensitive to the softening of the equation of state near a first order phase transition
- The behavior at mid-rapidity is highly linear, thus an important characteristic is the slope $v_1$ w.r.t rapidity

$$v_n = \langle \cos(n(\phi - \Psi_r)) \rangle$$

# Hadronic Transport Model Calculations

- Using JAM Model
- Centrality defined using $N_{part}$
- Rapidity dependent flow evaluated for $0.4<p_T<3.0$ GeV (as in data)

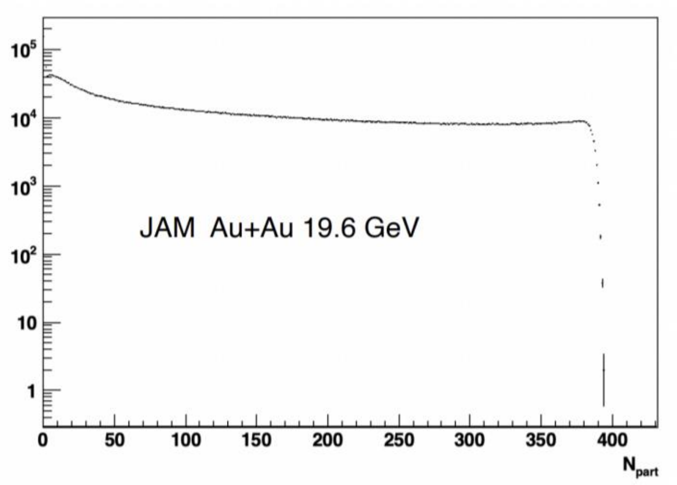


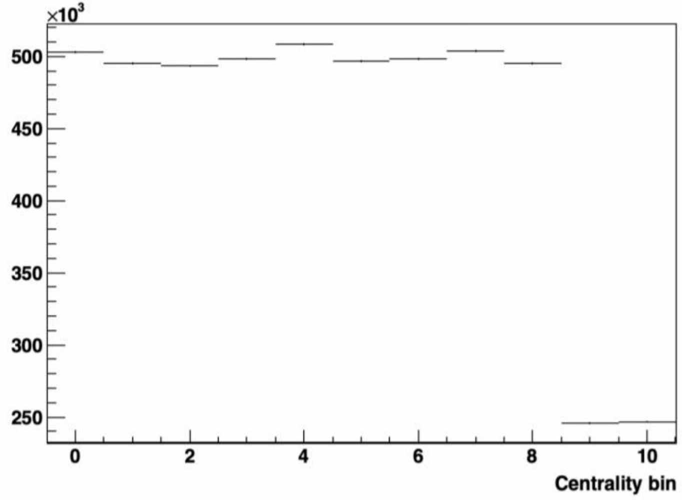


$$e = \int d^3p E^* f(p) + \frac{1}{2} m_\omega^2 \omega^2 + U(\sigma) \qquad m^* = m - S = m - g_s \sigma \qquad U(\sigma) = \frac{m_\sigma^2}{2}\sigma^2 + \frac{g_2}{3}\sigma^3 + \frac{g_3}{4}\sigma^4$$

RMD EoS, K = 210 MeV, Y. Nara et al. Phys. Rev. C 100, 054902 (2019)

# Modeling Collision Medium Behavior

- JAM Cascade mode, looking at spatial distributions at early times
- Radial distribution of all particles at given rapidities